Friday, July 31, 1998
REFRACTORY INCLUSIONS AND EVAPORATION PROCESSES
8:30 a.m. Walton Theatre

Chairs: R. H. Nichols Jr.
H. C. Connolly Jr.

Wood J. A.*
Constraints Placed by Aluminum-26 on Early Solar System History

McKeegan K. D.* Leshin L. A. MacPherson G. J.
Oxygen-Isotopic Stratigraphy in a Vigarano Type A Calcium-Aluminum-rich Inclusion

Young E. D.* Russell S. S.
Implications of In Situ Oxygen-Isotopic Microanalysis of an Allende Type B Calcium-Aluminum-rich Inclusion by Ultraviolet Laser Ablation and Gas Chromatography Isotopic Ratio Monitoring

Ito M.* Yurimoto H. Nagasawa H.
Oxygen-Isotopic Microanalysis of Calcium-Aluminum-rich Inclusions in Allende Meteorite: Intermineral and Intramineral Distribution

Hiyagon H.* Hashimoto A.
An Ion Microprobe Study of Oxygen Isotopes in Murchison (CM2) and Yamato 86009 (CV3) Chondrites: Discovery of Olivine Inclusions with Large Oxygen-16 Excess

Connolly H. C. Jr.* Burnett D. S.
Recycling (?): Relict Spinels(?) in Type B Calcium-Aluminum-rich Inclusions

Schirmeyer S.* Bischoff A.
Iron-Phyllosilicates in Calcium-Aluminum-rich Inclusions from CM Chondrites: Formation by Preaccretionary Alteration

Russell S. S.* Franchi I. A. Verchovsky A. B. Ash R. D. Pillinger C. T.
Carbon, Nitrogen, and Noble Gases in a Vigarano Calcium-Aluminum-rich Inclusion: Evidence for Silicon Carbide in Refractory Inclusions

Simon S. B.* Davis A. M. Grossman L.
Hibonite in Allende and Murchison Refractory Inclusions and Implications of the Absence of Cerium Depletions

Sahijpal S. Davis A. M. Goswami J. N.*
Isotopic and Trace-Element Abundances in Murchison Hibonites

Hashimoto A.*
Absolute Reaction Rates of Hydrogen with Condensed Phases in the Nebula

Davis A. M.* Hashimoto A. Richter F. M.
Isotopic Mass Fractionation Under Solar Nebular Conditions

Nagahara H.* Ozawa K.
Chemical and Isotopic Fractionation During Evaporation of a Multicomponent System

Nichols R. H. Jr.* Grimley R. T. Wasserburg G. J.
Measurement of Gas-Phase Species During Langmuir Evaporation of Forsterite

Esat T. M.* Williams I. S.
Rayleigh Distillation and Condensation of Potassium Isotopes

CONSTRAINTS PLACED BY ALUMINUM-26 ON EARLY SOLAR SYSTEM HISTORY.

J. A. Wood, Smithsonian Astrophysical Observatory, 60 Garden Street, Cambridge MA 02138, USA (jwood@cfa.harvard.edu).

The temporal constraint commonly associated with ^{26}Al is that some CAIs and Ca-rich chondrules, which contain no evidence of ^{26}Al, formed (presumably in the nebula) ≥5 Ma later than other CAIs that have radiogenic ^{26}Mg. However, different constraints emerge if it is acknowledged that ^{26}Al was the source of the heat that metamorphosed and melted the meteorite parent bodies, as it must have been.

1. The meteorite parent bodies must have accreted before 3 Ma (relative to t = 0 when ^{26}Al/^{27}Al in some CAIs was ~5×10^{-5}) in order to have inherited enough ^{26}Al to be significantly heated. This is inconsistent with the chronological interpretation of the ^{26}Al data summarized in the first paragraph; there must be some other explanation for the observed distribution of ^{26}Al in chondrite components.

2. In particular Vesta, the presumed HED parent body, must have accreted within ~1 Ma after t_0 for ^{26}Al to be able to generate enough heat to melt the HED magmas.

3. The volatility fractionation that strongly depleted ^{87}Rb in eucrites occurred over a period from 5 to 12 Ma after t_0 (allowing for the two eucrite subclasses, and uncertainty in initial ^{87}Sr/^{86}Sr). The fractionating event cannot have been condensation from the nebula, since this would have delayed accretion until ^{26}Al was practically extinct. The eucrites must have been devolatilized in some other way, after accretion and melting, presumably by loss to space upon eruption.

4. Aluminum-26 heating allows the time window in which ordinary chondrite parent bodies accreted to be rather narrowly defined: too soon, and they would have melted, as the HED parent body did; too late and they would not have reached the metamorphic temperatures indicated by mineral compositions. Accretion ~2 Ma after t_0 would have allowed ^{26}Al decay to raise deep interior temperatures in the chondrite parent bodies modelled by [1] to ~1000 K. Thus although we are conditioned to think of chondrites as the oldest samples of planetary material, in fact the achondrite, iron, and stony-iron parent bodies formed earlier than the chondrite parent bodies.

The points made in 2. and 4. are based on thermal evolution studies made by me (and by [1]). To the extent that ^{26}Al/^{27}Al for mean early solar system material was less than the value of 5×10^{-5} associated with a subset of CAIs, the events named above are require to have happened at even earlier times.

References: [1] Bennett M. E. and McSween H. Y. Jr. (1996) *GCA, 31*, 783-792.

OXYGEN ISOTOPE STRATIGRAPHY IN A VIGARANO TYPE-A CAI. K. D. McKeegan[1], L. A. Leshin[1], and G. J. MacPherson[2], [1]Department of Earth and Space Sciences, University of California-Los Angeles, Los Angeles CA 90095-1567, USA (kdm@ess.ucla.edu), [2]Department of Mineral Sciences, NHB-119, Smithsonian Institution, Washington DC 20560, USA.

The oxygen isotopic compositions of CAIs from CV meteorites are highly unequilibrated over a size scale of microns [1, 2]. This isotopic heterogeneity is thought to reflect partial isotopic exchange of the ^{16}O-rich inclusion with an external reservoir, where the degree of isotopic equilibration is dependent on diffusion rates in each mineral phase. Most oxygen isotopic measurements have been made on CAIs from Allende, many of which have abundant secondary minerals such as nepheline, sodalite, and grossular [3]. CAIs in the reduced CV chondrite Vigarano show little evidence for such secondary alteration [4]. Clayton et al. (1987) found that 4 Vigarano CAIs have bulk oxygen isotopic compositions that fall at intermediate values along the Allende mixing line and inferred that the oxygen isotopic exchange process in Allende CAIs is not related to secondary mineralization [5]. We have used the UCLA ims 1270 ion microprobe to analyze δ^{18}O and δ^{17}O in 21 spots of one of these four inclusions. Measurements were made with a spatial resolution of ~10μm in all major mineral phases in the inclusion and its surrounding rim sequence.

Vigarano 1623-2 is a type A inclusion that consists largely of melilite, with intergrown spinel and hibonite predominantly in the central regions [4]. Minor phases include perovskite and Fe-Ni metal. The inclusion is rimmed by a nearly continuous Wark-Lovering (WL) sequence consisting of spinel, Ti-rich clinopyroxene (fassaite), and aluminuous diopside. Surrounding the WL rim is a layer rich in forsteritic olivine interpreted to be an accretionary rim [6].

The oxygen isotope data scatter along the Allende CAI mixing line (Fig. 1) with spinel and hibonite ^{16}O-enriched to 'typical' values of –40 to –50‰ and melilite plotting near the ^{16}O-depleted end of the mixing line. Although there is some isotopic heterogeneity between melilite grains, no systematic difference with location is apparent, i.e. the compositions for grains from the inclusion interior overlap the range observed for grains just beneath the rim. Four rim traverses were made taking care to analyze nearly pure mineral phases. Rim spinel is isotopically indistinguishable from interior spinel grains. In the pyroxene layer, oxygen isotopes are correlated with Ti content in that fassaite (single analysis) shows a high ^{16}O-enrichment comparable to spinel while diopside is characterized by intermediate ^{16}O-excesses. Analyses of olivine grains in the accretionary rim demonstrate a clear ^{16}O-enrichment of just a few permil less than that measured in spinel.

Fig. 1. Oxygen isotope compositions of individual minerals in Vigarano 1623-2 and its rim are plotted with 1σ error bars. The Allende CAI mixing line and the terrestrial fractionation lines are shown for reference. Bulk data for Vigarano 1623-2 are from Clayton et al [5].

The similarity of melilite isotopic compositions between essentially unaltered Vigarano 1623-2 and Allende inclu-

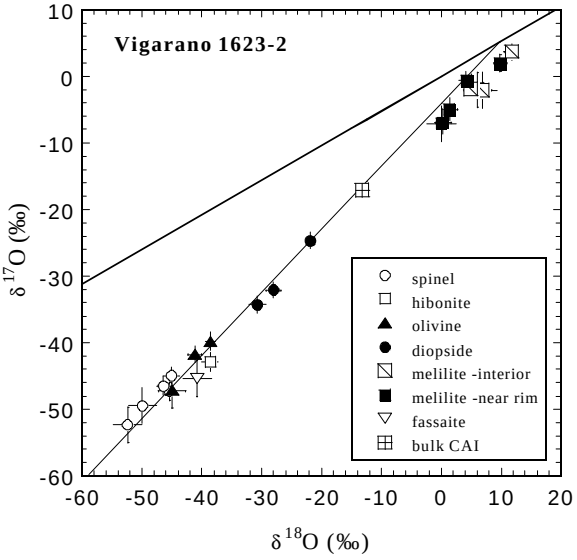

sions demonstrates that oxygen isotopic exchange in melilite is not necessarily accompanied by secondary mineralization. Our analyses of rim sequences corroborate recent ion microprobe measurements of rims on 2 Allende CAIs [7], except that in Vigarano 1623-2 the olivine in the accretionary rim is even more highly ^{16}O-enriched. The preservation of large ^{16}O-enrichments in fine-grained phases in the WL and accretionary rims indicates that any possible parent body alteration is not likely to have affected CAI nebular oxygen isotopic patterns. In agreement with previous Mg isotope measurements [8], the apparent lack of isotopic mass fractionation argues against evaporation from a melt as being an important mechanism for WL rim formation [9, 10].

References: [1] Clayton R. N. et al. 91977) *EPSL, 34,* 209–224. [2] McKeegan K. D. et al. (1996) *Meteoritics & Planet. Sci., 31,* A86–A87 (1996). [3] MacPherson G. J., Wark D. A., and Armstrong J. T. (1988) in *Meteorites and the Early Solar System* (Kerridge and Matthews, eds.) pp. 746–807. [4] Mao X.-Y. (1990) *GCA, 54.* [5] Clayton R. N. (1987) *LPS XVIII,* 185–186. [6] MacPherson G. J., Hashimoto A., and Grossman L., (1985) *GCA, 49,* 2267–2280. [7] Hiyagon H. (1998) *LPS XXIX,* Abstract #1582. [8] Davis A. M. and MacPherson G. J., *Meteoritics, 29,* 458–459. [9] Ruzicka A. and Boynton W. V. (1994) *Meteoritics, 29,* 526. [10] Wark D. A. (1997) *Meteoritics & Planet. Sci., 32,* A135.

IMPLICATIONS OF IN-SITU OXYGEN ISOTOPE MICROANALYSIS OF AN ALLENDE TYPE B CAI BY UV LASER ABLATION AND GAS CHROMATOGRAPHY ISOTOPE RATIO MONITORING. Edward D. Young, *Department of Earth Sciences, University of Oxford, Oxford OX1 3PR, UK, ed.young@earth.ox.ac.uk*, Sara S. Russell, *Department of Mineralogy, The Natural History Museum, Cromwell Road, London SW7 5BD, UK, sarr@nhm.ac.uk.*

The linear array defined by calcium-aluminum-rich inclusions (CAIs) from CV meteorites on a plot of δ^{17}O vs δ^{18}O is commonly described as defining a slope of "nearly one" to contrast it with mass fractionation slopes slightly greater than 0.5. The actual slope of the line as presently defined (the CCAM) is 0.94 ± 0.02 and was determined with high precision by fluorinating mineral separates and analyzing the liberated oxygen by gas-source isotope ratio mass spectrometry [1].

Lack of colinearity among ordinary chondrites (OC), the ^{16}O-enriched components of CAIs, and the intersection of the CCAM line with the terrestrial mass fractionation line (figure 1), together with the relative positions of other solar system bodies on the three-isotope plot, has been used as evidence that there must have been 3 or more oxygen reservoirs during planetesimal formation in the early solar nebula [2]. New high-precision laser-ablation oxygen isotope analyses of a type B CAI from the Allende meteorite (figure 1) suggest that there were no more than 2 nebular oxygen reservoirs.

Twenty-two analyses of Allende inclusion USNM 3576-1 were obtained with a spatial resolution of 100 μm and an analytical precision of ± 0.2 per mil using a new method that combines *in-situ* UV laser ablation and fluorination with gas-chromatography isotope ratio monitoring. Accuracy and precision of the method were validated by analyzing terrestrial standards and a smaller Allende CAI. Inclusion 3576-1 (2 x 0.5 cm) yields a Pb-Pb age of 4.566 Ga [3].

Data for primary fassaite, spinel, and melilite (melilite, open symbols in figure 1) lie along a linear array with a best-fit slope of 1.00 ± 0.03 ($r = 0.9998$). Data for melilite within 100 μm of the inclusion rim that has been partially replaced by micron to submicron intergrowths of feldspar (An_{88}) + nepheline ± clinopyroxene (closed symbols, figure 1, $n = 6$), as well as for melilite analyses that also include secondary minerals in the inclusion interior adjacent fassaite (three of the closed symbols in figure 1), comprise a mass-fractionation trend toward heavy isotope enrichment. Mixtures between altered melilite and spinel form a chord similar to the CCAM line. Distinction between the slope 1 line and the CCAM will have gone undetected until now because alteration of melilite can be incipient and difficult to detect in mineral separates while SIMS methods lack the required analytical precision.

It is suggested that a single line (line 2, figure 1) with a slope of exactly one, represented by primary CAI phases and OC components, defines the primitive oxygen isotope reservoir of the nebula. Virtually all other planetary and meteoritic bodies are enriched in ^{17}O and ^{18}O relative to this line and their oxygen isotope ratios can be explained by mass fractionation initiating from it. The simplicity of the proposed primordial array with slope of 1.00 argues for its validity; it is more consistent with either mixing of a pure ^{16}O stellar component with nebular oxygen or unmixing by non-mass dependent gas-phase reactions than are slopes less than one (e.g., the CCAM) and it links the most abundantly sampled representative of primitive rock-forming oxygen in the nebula, OCs, with the clearly primitive ^{16}O-rich component of CAIs.

References: [1] Clayton R.N. et al. (1977) *EPSL*, 34, 209-224. [2] Clayton R.N. and Humayun M. (1994) *Min. Mag.*, 58A, 177-178. [3] Manhès G. et al. (1988) *Compt. Rend. Planét.*, 323-327.

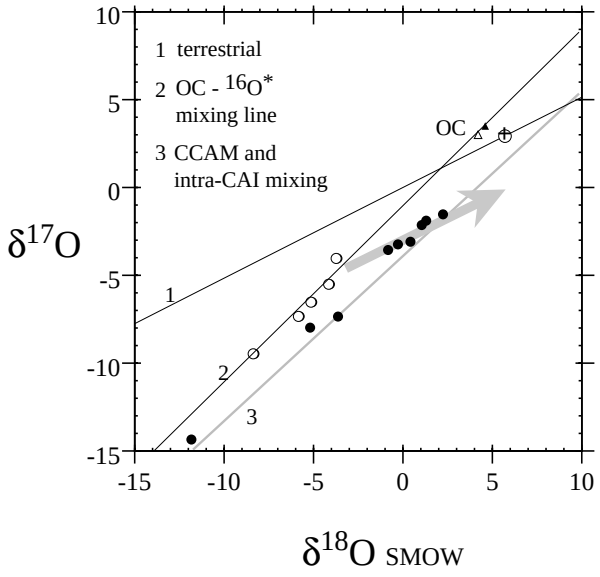

OXYGEN ISOTOPE MICRO-ANALYSIS OF CALCIUM-ALUMINUM-RICH INCLUSIONS IN ALLENDE METEORITE: INTER/INTRA-MINERAL DISTRIBUTION. M. Ito[1], H. Yurimoto[2], and H. Nagasawa[1], [1]Department of Chemistry, Gakushuin University, Mejiro, Toshima-ku, Tokyo 171-8588, Japan (96242001@gakushuin.ac.jp, hiroshi.nagasawa@gakushuin.ac.jp), [2]Department of Earth and Planetary Sciences, Tokyo Institute of Technology, Ookayama, Meguro-ku, Tokyo 152-8551, Japan (yuri@geo.titech.ac.jp).

Introduction: The O isotope composition of 7R-19-1 (a), a compact Type A CAI from Allende meteorite, were measured by secondary ion mass spectrometry (SIMS) with a high mass resolution *in-situ* determination technique. In this paper some new data, in addition to those reported in [1], are presented and discussed. We measured micro-distributions of oxygen isotopes within two melilite single crystals with similar gehlenite - åkermanite ratio and at the boundary of the two melilite crystals.

Sample Description: The sample used in this study was a polished section, 7R-19-1 (a) from 7R-19-1 the coarse-grained compact Type A CAI in the Allende meteorite. Petrographically 7R-19-1 consists of melilite ($Åk_{13\text{-}30}$, roughly 60 ~70 %), fassaite (~10 %) and spinel (~10 %) grains and, the rim fringed with sodalite.

Experimental Procedure: The polished samples was coated with 30 nm gold film for SIMS analysis in order to eliminate the electrostatic charge on the sample surface. Oxygen isotope ratios were measured by the T.I.Tech ims CAMECA 1270 SIMS instrument with a high mass resolution technique. The primary ion beam was massfiltered positive ^{133}Cs ions accelerated to 10 keV and beam spot size of ~3 µm in diameter. Negative secondary ions of ^{16}O tail, ^{16}O, ^{17}O, ^{16}OH and ^{18}O were detected by an electron multiplier (EM) operated in a pulse counting mode. A mass resolution power was set to ~6000, sufficient to completely eliminate hydride interference in order to resolve $^{17}O^-$ from mass interference of $^{16}OH^-$. The basic conditions for oxygen isotope measurement are described in the previous work in detail [1]. The matrix effect which may cause inter-mineral systematic errors were checked by comparing the analytical results for terrestrial analogues. The instrumental mass fractionation was checked by measuring oxygen isotope ratios of terrestrial standards with known oxygen isotopic ratios [2].

Results and Discussion: The results are plotted in a three isotope diagram which is shown in Fig 1. The values of melilite, fassaite and spinel for 7R-19-1(a) fall on the carbonaceous chondrite anhydrous minerals (CCAM) line. Melilite#2, spinel and fine-grained fassaite in melilite#2 showed large negative anomaly of about -30 to -40 ‰. Melilite#1, fine-grained fassaite in melilite#1 and blocky fassaite showed smaller negative anomaly of about 0 to -20‰. The fine-grained fassaite in melilite crystals appear to have the same origin as the surrounding melilite since O isotopic ratios are similar. The observed inter-distributions of O isotopes are differ significantly from the normal type-B1 CAI's in the Allende meteorite, but are rather the those observed by previous work [3]. The åkermanite composition in melilite#1 and #2 are similar. The oxygen isotope profiles were obtained from stepped linear traverses across the boundary of two melilite crystals #1 and #2. The measurement consisted of 8 points at intervals of 15 µm. Oxygen isotopic composition distributed homogeneously within each melilite crystal, but the isotope composition was abruptly changed at the boundary.

References: [1] Ito, M. et al. (1998) LPS, **29**, #1556. [2] Yurimoto, H. et al. (1994) EPSL, **128**, 47-53. [3] Kim, G. L. et al. (1998) LPS, **29**, #1344. [4] Clayton, R. N. (1993) Annu. Rev. Earth Planet. Sci., **21**, 115-149.

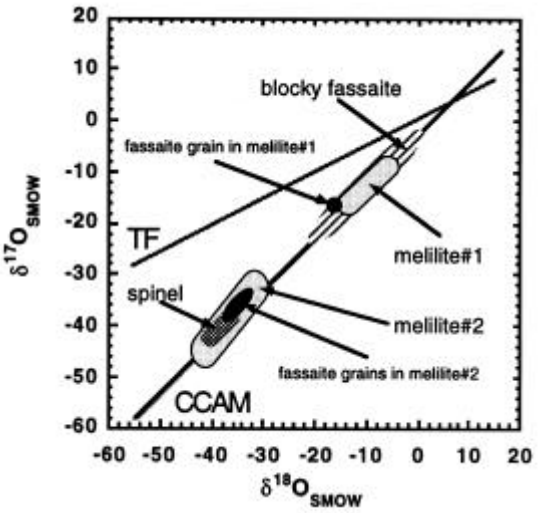

Fig 1. Oxygen isotopic compositions of 7R-19-1 (a) from Allende meteorite. Terrestrial fractionation (TF) line and carbonaceous chondrite anhydrous mineral mixing (CCAM) line defined by [4] were presented.

AN ION MICROPROBE STUDY OF OXYGEN ISOTOPES IN MURCHISON (CM2) AND YAMATO-86009 (CV3) CHONDRITES: DISCOVERY OF OLIVINE INCLUSIONS WITH LARGE OXYGEN-16 EXCESS. H. Hiyagon[1] and A. Hashimoto[2], [1]Department of Earth and Planetary Physics, The University of Tokyo, Bunkyo-ku, Tokyo 113, Japan (hiyagon@geoph.s.u-tokyo.ac.jp), [2]Department of the Earth and Planetary Sciences, Hokkaido University, Sapporo 060, Japan.

In order to understand the origin of oxygen isotopic anomalies in the early solar system, it is critical to determine micro-distributions of oxygen isotopes in various petrographic components inside various types of meteorites. As a first step of such extensive studies, we have performed *in situ* oxygen isotope analyses of Murchison (CM2) and Yamato-86009 (CV3) chondrites using a CAMECA ims-6f ion microprobe at the University of Tokyo.

Samples: Four olivine-rich inclusions (Y86009-A, -B, -C, and -D), one spinel-pyroxene-feldspar aggregate (-E) and one chondrule (-F) in a thin section of Yamato-86009 (CV3) chondrite, and four olivine-rich inclusions (MC5a-52, -47, -26 and -94) and one chondrule (-85) in a thin section of Murchison (CM2) chondrite have been investigated. The olivine-rich inclusions in both meteorites consist predominantly of Mg-rich olivine (Mg/[Mg+Fe] =97-98 mol% for Y86009-A and -C, and >99 mol% for others), and of variable amounts (~1% to ~50% by volume) of interspersed, Ca-Al-rich domains (~10-50 μm accross; mostly diopsidic or fassaitic pyroxene with or without spinel) being enclosed by olivine. The inclusions are irregular but generally lumpy in shape, and have numerous, irregularly-shaped voids (sub-μm to a few μm in size) both in olivine and Ca-Al-rich areas. From their outlook, they are probably amoeboid olivine aggregates. Chondrule #F consists of forsterite, enstatite, diopside and glass; chondrule #85 consists of forsterite, enstatite and a minor amount of diopside. (See [1] for details of Y-86009.) A Cs^+ primary beam of ~15μm diameter (or ~30 μm dia. for an olivine grain of chondrule #F) was used in the ion microprobe analyses. Analytical conditions were similar to those described in [2].

Results: All the 13 analyses made on olivine grains inside the olivine-rich inclusions show ^{16}O-enrichments with both $\delta^{17}O$ and $\delta^{18}O$ values from -40‰ to ~-50‰. This is the first observation of olivine that has oxygen isotopic compositions at lower ends of the slope ~1 correlation line in the $\delta^{17}O$ vs $\delta^{18}O$ diagram, which was defined by many analyses of Allende CAI minerals [3,4]. The fassaite-diopside-rich phase in the same olivine-rich inclusions also show high high excesses in ^{16}O ($\delta^{17}O$ and $\delta^{18}O$ from -32‰ to -42‰). The olivine-rich inclusions are abundant in these meteorites; in fact, at least 10 and 40 olivine-rich inclusions of similar morphologies are observed in the thin sections of Y-86009 (5mm x 5mm) and Murchison (6mm x 7.5mm), respectively. A monomineralic spinel grain and spinel+pyroxene areas of the spinel-pyroxene-feldspar aggregate (Y86009-E) show high anomalies ($\delta^{17}O \sim \delta^{18}O < -40‰$), while feldspar-rich areas in the same inclusion show normal compositions ($\delta^{18}O$ from +6 to +8‰). The chondrules (#F and #85) also show some ^{16}O enrichments ($\delta^{18}O$ from -12‰ to -4‰).

The result suggests that fromation of olivine-rich inclusions involved the same process (or source) which resulted in oxygen isotopic anomalies in CAIs. It implies that the oxygen isotopic anomaly was more extensive in the early solar system than we thought previously. The present work is only the beginning of our extensive survey on various types of petrographic components from different meteorites. We believe that *in situ* isotopic studies will provide unprecedented information regarding not only the cause of oxygen isotopic anomalies, but also the origin of CAIs, olivine-rich inclusions, chondrules, and their relationships.

References: [1] Hiyagon H. and Hashimoto A. (1998) *Antarct. Meteorites* 23 (NIPR Symp. abstr., submitted). [2] Hiyagon H. (1998) *LPS XXIX*, 1582–1583. [3] Clayton R. N., Grossman L., and Mayeda T. K. (1973) *Science, 182,* 485–488. [4] Clayton R. N., Onuma N., and Mayeda T. K. (1976) *EPSL, 30,* 10–18.

RECYCLING (?); RELICT SPINELS (?) IN TYPE B, CAIS. H. C. Connolly Jr. and D. S. Burnett, Division of Geological and Planetary Sciences, Mail Code 100-23, California Institute of Technology, Pasadena, CA 91125.

Type B CAIs can be thought of as a type of chondrule despite obvious differences in size, composition and textures. Nevertheless igneous CAIs likely experienced similar thermal histories. A major constraint on the thermal history of chondrules is that they have been recycled, mainly supported by the presence relict grains. Although well known that igneous CAIs experienced at least two melting events (counting Wark-Lovering rims), the identification of relict grains has been problematic.

The best candidate for relict grains within type B's is spinel. Spinel is the liquidus phase with complete melting at approximately 150°C above type B peak melting temperatures (~1400°C). Consequently, relict spinels, either from a previous generation of CAIs or direct nebular condensate spinels are stable at the inferred maximum heating temperature of type B CAIs. Minor and trace element concentrations can be used to distinguish relict grains from those that crystallized from an initially homogeneous liquid.

We measured minor element concentrations in spinels from two type B, CAIs, Allende TS-23 and Leoville 3537-2 (6). Our results show that Ti and V are positively correlated, but their concentrations vary as a function of the petrologic location and context. Grains located in the edge areas form a separate population from grains in the center. Edge areas are richer in V than Ti (~0.16–0.44 wt% and ~0.06–0.25 respectively). Spinels enclosed within melilite, define a different pattern from those enclosed by fassaite (overall range ~0.09–0.33 wt% V and ~0.06-0.40 wt% Ti). Experiments show that spinel crystallization effectively ceases before 40–50% total crystallization. As Ti is highly incompatible in this part of the crystallization sequence, at most a factor of 2 range within spinel is expected from fractional crystallization. Our data show a range from 3 (TS-23) to 6 (Leoville) in Ti concentrations, inconsistent with fractional crystallization.

If a population of spinels were truly "relict", because they were produced in some other generation of CAI which was broken and spinels then reaccreated into the precursor of the two studied objects, their apparent correlations between minor element contents and host mineral should not exist. Their distribution within the CAI should be random. The presence of a petrologic correlation suggests that another process dominated. It may be that the various populations of spinels were generated in a remelting event(s).

If the objects were remelted to temperatures between 1200°–1250°C, a liquid dominated by melted cpx would be produced. This cpx-rich liquid would be enriched in Ti over the bulk composition. Such a Ti-rich liquid could introduce Ti into existing spinels through diffusion. It is also possible that the new liquid (pyx-rich and/or pyx+an-rich) would not be spinel saturated. Upon cooling, these liquid pockets would first produce spinels, containing a higher Ti concentration than existing spinels trapped in melilite, as observed in out data set.

Edge spinels have V and Ti concentrations different from the middle and center regions as well as lower Cr and higher Fe abundances. Although the high Fe may reflect some secondary alteration process, the other elements appear unaffected. Furthermore, the Fe and Cr concentrations do not match predictions (Ebel and Grossman, private comm.) so they are apparently not condensates. We suggest that these grains are a later generation due to the melting of mantle melilite. It is possible that the Wark-Lovering rim forming process was more extensive than previously believed.

In summary, it appears that remelting more than one generation of spinels for both CAIs studied. We have no evidence for any true "relict" spinels.

IRON-PHYLLOSILICATES IN CALCIUM-ALUMINUM-RICH INCLUSIONS FROM CM CHONDRITES: FORMATION BY PREACCRETIONARY ALTERATION. S. Schirmeyer and A. Bischoff, Institut für Planetologie, Wilhelm-Klemm-Strasse 10, 48149 Münster, Germany (schirms@nwz.uni-muenster.de).

Introduction: Phyllosilicates (e.g., serpentine, cronstedtite) are widespread in CM-chondrites. These minerals are essential components of the accretionary dust rims and the host rock [1]. Additionally, they also occur as alteration phases in CAIs [2,3] and chondrules [4]. It is generally accepted that most CAIs and chondrules in CM chondrites were altered by aqueous processes, however, time and location of aqueous processing is discussed controversely. Some features like the presence of Ca-sulphate veins in Cold Bokkeveld can only be explained by parent body alteration [5]. Clear evidence for pre-accretionary aqueous alteration (i.e. in the solar nebula or in short-lived precursor planetesimals) also exists [6–9].

Results and discussion: In this study 14 CAIs from Yamato 791198 (2), Banten (4), Murchison (5), and Cold Bokkeveld (3) were examined. In many cases CAIs contain a Fe-phyllosilicate rim sited between the spinel bearing core and the outermost pyroxene rim (Wark-Lovering rim). It is believed that this secondary, phyllosilicate-rich rim is replacing completely altered melilite [10]. Significant differences in mineralogy and chemistry between these "CAI-rims" and the secondary products of the adjacent so-called "matrix" exist and have been described recently (e.g., enrichment of Li in the inner "CAI-rim" [7,8]).

In other CAIs the outer pyroxene rim is completely missing (Fig. 1), probably due to fragmentation of the CAI and loss of the Ca-pyroxene rim prior to incorporation of the CAI into the final host chondrite. Based on many observations it appears that the Wark-Lovering rim of a CAI is susceptible for fragmentation, after formation of an inner Fe-phyllosilicate rim replacing melilite. There is no evidence that the melilite alteration has happened in the same process forming the Fe,Mg-phyllosilicates of the "matrix". This is indicated by fundamental differences in mineralogy and chemistry. One example is shown in Fig. 1. A spinel-rich CAI is completely surrounded by a phyllosilicate-rim having an extremely high concentration of Fe. Browning et al. [11] suggested that progressive aqueous alteration is accompanied by a continuous mineralogic trend from Fe^{3+}-rich cronstedtite to Mg-rich serpentine. Thus, the Mg/Fe-ratio of the "matrix"-phyllosilicates increases. But this is not the case for the alteration products of CAIs. Although Cold Bokkeveld shows the highest mineralogical alteration index [10], the Fe-phyllosilicate rim is in close contact to the adjacent Mg-rich phyllosilicates of the "matrix". No reaction zone is visible. We do not see any possibility to produce an Fe-rich "CAI phyllosilicate rim" in the same alteration process modifying the original "matrix" mineralogy and producing phyllosilicates with much higher Mg/Fe-ratios.

Conclusions: Formation of Fe-rich phyllosilicate by replacing melilite must have occurred prior to the loss of the Ca-pyroxene rim of the CAI and prior to the incorporation of the modified object into the final CM-rock. Therefore, a preaccretionary alteration scenario for the observed alteration features in CAIs is suggested.

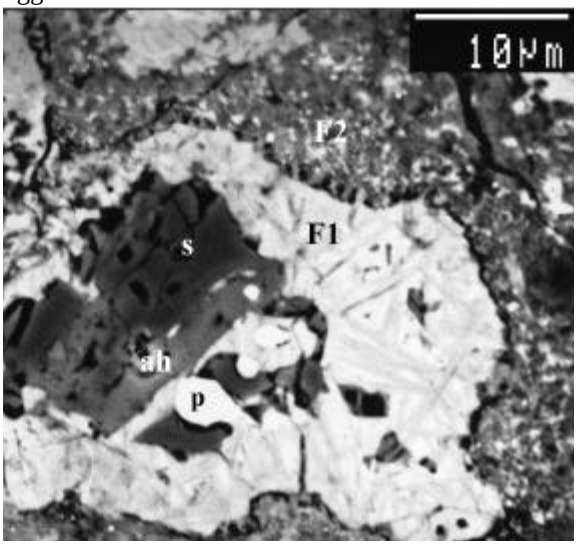

Fig. 1. Spinel-rich (s) Ca,Al-rich inclusion from Cold Bokkeveld with a thick rim of Fe-rich phyllosilicates (F1) in close contact with Mg-rich phyllosilicates (F2) of the bulk meteorite. Other constituents of this CAI are perovskite (p) and altered hibonite (ah).

References: [1] Zolensky M. E. et al. (1990) *LPS XXI*, 1249–1250. [2] Lee M. R. and Barber D. J. (1991) *Meteoritics, 26,* 362. [3] Lee M. R. and Greenwood R. C. (1994) *Meteoritics, 29,* 780–790. [4] Hanowski N. P. and Brearley A. J. (1997) *LPS XVIII*, 501–502. [5] Lee M. R. (1993) *Meteoritics, 28,* 53–62. [6] Metzler K. et al. (1992) *GCA, 56,* 2873–2897. [7] Schirmeyer S. et al. (1996) *LPS XXVII*, 1141–1142. [8] Schirmeyer S. et al. (1997) *LPS XXVIII*, 1253–1254. [9] Bischoff A. (1997) *LPI/TR–97–02, Part 1,* 2–3. [10] Greenwood R. C. et al. (1994) *GCA, 58,* 1913–1935. [11] Browning L. B. et al. (1996) *GCA, 60,* 2621–2633.

CARBON, NITROGEN AND NOBLE GASES IN A VIGARANO (CV) CAI: EVIDENCE FOR SILICON CARBIDE IN REFRACTORY INCLUSIONS. S. S. Russell[1], I. A. Franchi[2], A. B. Verchovsky[2], R. D. Ash[3], and C. T. Pillinger[2] [1]Department of Mineralogy, The Natural History Museum, Cromwell Road, London SW7 5BD, UK, [2]Planetary Sciences Research Institute, Open University, Milton Keynes, MK7 6AA, UK, [3]Geophysical Laboratory and Department of Terrestrial Magnetsim, Carnegie Institution, 5251 Broad Branch Road, Washington DC 20015, USA.

Introduction: Isotope anomalies are observed in CAIs, implying that they formed before isotopic homogenisation had been completed. Isotopic studies have concentrated on refractory elements (e.g., Ti, Ca), and O. The more volatile elements, although likely to be under-abundant in CAIs, may also shed some light on CAI precursor materials and formation mechanisms. Here we report the results of a pilot study into the abundance and isotopic composition of C, N and noble gases in CAIs from Vigarano (CV3). Vigarano was chosen as it contains large CAIs that have suffered less alteration than their counterparts in the more-studied Allende. The results were compared to C data previously obtained on an Allende CAI [1].

Technique: The interior of a CAI, VS2, was picked out from a slab of Vigarano using a needle. VS2 (4mm × 3mm) consists predominantly of melilite ($Ak_{\sim 5}$), with abundant spinel, hibonite laths (TiO_2 ~2%), and Fe-Ni beads and minor Al-rich diopside. Gases liberated from a stepped combustion extraction to 1400°C of 5.7mg of VS2 were analysed on an automated mass spectrometer system (FINESSE) for the abundance and isotopic composition of He, C, N, Ne and Ar.

Results: *Carbon:* Discounting C released below 500°C, which appears to be mainly terrestrial contamination, the C abundance of VS2 is ~100ppm, at the lower end of the range observed for chondrules [2]. The mean $\delta^{13}C$ is -12‰, approximately 6‰ heavier than bulk Vigarano [3], and is constant over a broad temperature range, suggesting most of the C is dissolved in silicates. A peak in $\delta^{13}C$ of -8 ± 1‰ at 550°C suggests the presence of minor carbonate (~10 ppm). In the highest temperature steps the $\delta^{13}C$ increases to -5 ± 1‰, consistent with the presence of SiC. A previously measured CAI from Allende released even heavier C at high temperatures ($\delta^{13}C = +29 \pm 1$‰, [1]).

Nitrogen: The bulk N content of the CAI is 16 ppm, calculated assuming only material released above 500°C is indigenous. Nitrogen is released over a wide temperature range. The mean $\delta^{15}N$ over the whole release is +17‰, distinguishable from bulk CV meteorites that yield $\delta^{15}N < 0$‰; $\delta^{15}N$ for Vigarano is –11‰ [3,4]. The difference in $\delta^{15}N$ between this CAI and bulk CV suggests that the CAI sampled isotopically distinct material or was subject to an evaporation event that caused fractionation of N (and perhaps C). In the highest temperature steps, a ^{14}N-rich component (minimum $\delta^{15}N = -53$‰) is released, that has similar combustion characteristics to presolar SiC.

Noble gases: Two main release peaks for He and Ar are observed, at 400°C and 700°C. Ar has a planetary isotopic signature. A small amount of cosmogenic ^{21}Ne is detected around 700°C. Over the highest temperature range no detectable noble gases are released, with the exception of ^{22}Ne at a level ~15% above blank. Such a signature is indicative of Ne-E.

Discussion: The C, N and Ne data suggest the presence of relict presolar SiC in VS2, indicating the reservoir from which CAIs formed contained presolar dust, some of which survived the CAI formation event without melting or degassing. Assuming CAI SiC has similar characteristics to that in the matrix, the abundance of SiC is estimated as 0.1 ppm from the C data, and 5 ppm from the N data. The small amount of ^{22}Ne detected suggests a value of a few parts per million, but with considerable uncertainty. The disparity in SiC abundance determinations from C and N may reflect the presence of components that are unaccounted for in our calculations. Alternatively, the CAI SiC may have a different mean N abundance or isotopic composition to matrix SiC. Whichever abundance estimate is correct, it appears that the SiC concentration in this CAI is of a similar order of magnitude, or higher, than the 0.2 ppm present in bulk Vigarano [5]. An estimate of the SiC abundance in an Allende CAI (1 ppm) [1] was also higher than in bulk Allende (0.01 ppm, [5]). Together these data suggest the CAI formation region may, in fact, have been enriched in presolar SiC.

References: [1] Ash and Russell (1994) in *Chondrules and the Protoplanetary Disk* (R. H. Hewins et al., eds.) p. 2, Cambridge Univ. [2] Hanon et al. (1995) *Meteoritics, 30,* 516. [3] Kerridge (1985) *GCA, 49,* 1707. [4] Chung and Clayton (1978) *EPSL, 38,* 421 [5] Russell et al. (1992) *Meteoritics, 27,* 283.

HIBONITE IN ALLENDE AND MURCHISON REFRACTORY INCLUSIONS AND IMPLICATIONS OF THE ABSENCE OF CERIUM DEPLETIONS. S.B. Simon[1], A. M. Davis[1,2], and L. Grossman[1,2], [1]Department of the Geophysical Sciences, 5734 South Ellis Avenue, University of Chicago, Chicago IL 60637, USA (sbs8@midway.uchicago.edu), [2]Enrico Fermi Institute, University of Chicago, Chicago IL 60637, USA.

Introduction: We have studied two hibonite-rich fluffy Type A (FTA) inclusions, ALH2 and ALH3, from Allende and SH-6, a fluffy, hibonite-spinel inclusion from Murchison. Although it is very likely that these types of inclusions are primary condensates [1,2], their trace element abundances have not been thoroughly studied. We analyzed hibonite and melilite in the two FTAs and hibonite in SH-6 with the ion microprobe to determine the trace element abundances of (presumed) condensates; to compare the trace element contents of Allende hibonite with those of Murchison hibonite; and to see if Allende hibonite exhibits negative Ce anomalies, as would be expected if its very low Ti^{3+}/Ti^{tot} ratios and orange color reflect condensation under oxidizing conditions rather than later equilibration [3].

Samples: Inclusion ALH2 has melilite up to 200 µm across and hibonite plates up to ~50 µm across. ALH3 has coarser melilite (up to 700 µm) and is less altered than ALH2. The outer ~400 µm of ALH3 consist of melilite with sparse spinel and perovskite, but the interior has zones that are very rich in hibonite and spinel. Melilite is very aluminous ($Åk_{0.5–20}$) and hibonite has 2–7 wt% TiO_2. Most hibonite plates are 20–40 µm across and are subhedral to anhedral. Sample SH-6 has a porous core of blue, euhedral hibonite plates that are 2–10 µm across, and an ~10 µm thick rind of spinel. It was described by [2].

Results: Both SH-6 and ALH3 have Group II chondrite-normalized REE patterns. This is seen in both the hibonite and melilite of ALH3, indicating a common source for these phases. ALH2 has a flat pattern, probably a Group I. The hibonite in ALH2 and ALH3 has no Ce anomalies, supporting the previous suggestion [3] that the oxidizing conditions inferred for Allende hibonite reflect reequilibration rather than condensation under extremely oxidizing conditions. The ALH2 and ALH3 hibonite REE patterns are quite different from each other and from most Murchison hibonites that have been analyzed [4]. While Murchison hibonite commonly has flat light REE (LREE) abundances at ~100 × CI, hibonite in ALH2 has very low LREE abundances, ~5 × CI. In ALH3 hibonite, LREE abundances are not flat but instead fall by 2–3× from La (40–80 × CI) through Sm, then drop off even more sharply, at least through Gd, at 2–10 × CI. As is typical of Group II patterns, Tm is enriched relative to the refractory heavy REE (HREE), but the latter could not be measured accurately because of interferences due to the high LREE/HREE ratios and low concentrations. Yttrium, an element that is as refractory as Lu, is also very low, ~1×CI.

Discussion: Most hibonite-, spinel-bearing inclusions are thought to have last equilibrated with the nebular gas at 1200°–1230°C [5]. Under conditions sufficiently oxidizing to form orange hibonite, Ce is quite volatile relative to the other REE at these temperatures [6]; yet no Ce depletions are observed in ALH2 or ALH3. It is unlikely that the Allende hibonite formed under oxidizing conditions and that Ce eventually completely condensed into it because equilibration temperatures much lower than those found by [5] would be required. It is also unlikely that Ce condensed into another phase and was later redistributed within ALH2 and ALH3 in just the amounts required to erase anomalies. We agree with the previous suggestion [3] that Allende hibonite formed under "normal", reducing conditions (*i.e.*, without Ce depletions) and was later altered at higher oxygen fugacities to produce its orange color. Experiments [3] have shown that blue, Ti^{3+} -bearing hibonite can become orange in one hour at 1430°C at an fO_2 of 10^{-8}, indicating that Ti^{3+} in hibonite can oxidize easily at high temperatures. From the above observations, we conclude that it is likely that Allende hibonite was altered under oxidizing conditions at elevated but subsolidus temperatures, probably in the nebula. In contrast, Murchison inclusions, which contain oxidized secondary phases such as Fe-bearing phyllosilicates, yet retain blue hibonite, must have experienced much lower alteration temperatures than did Allende inclusions. A study of the time required at various temperatures for the blue-to-orange transition in hibonite would likely place valuable constraints on the alteration conditions experienced by all hibonite-bearing inclusions.

References: [1] MacPherson G. J. and Grossman L. (1984) *GCA, 48*, 29. [2] MacPherson G. J. et al. (1984) *Proc. LPSC 15*, *JGR*, C299. [3] Ihinger P. D. and Stolper E. (1986) *EPSL, 78*, 67. [4] Ireland T. et al. (1988) *GCA, 52*, 2841. [5] Beckett J. R. and Stolper E. (1994) *Meteoritics, 29*, 41. [6] Davis A. M. et al. (1982) *GCA, 46*, 1627.

ISOTOPIC AND TRACE ELEMENT ABUNDANCES IN MURCHISON HIBONITES. S. Sahijpal[1], A. M. Davis[2], and J. N. Goswami[1], [1]Physical Research Laboratory, Ahmedabad-380 009, India, [2]Enrico Fermi Institute, University of Chicago, Chicago IL 60637, USA.

Two platy hibonite crystals and hibonites from two spinel-hibonite inclusions (an irregular chip and a spherule) from the Murchison meteorite were analysed for their titanium and calcium isotopic compositions and trace element abundance patterns. All the samples were hand-picked from an HF-HCl resistant residue of a large piece of Murchison meteorite. The measurements were carried out by a Cameca ims-4f ion microprobe using standard procedures [1].

Both of the platy hibonites, B3 and B5, have Group III REE patterns with negative Eu and Yb anomalies and a smooth roll-over in the abundances of HREE (Fig. 1). These features are typical of platy Murchison hibonites [1,2]. Excess ^{50}Ti is present in both hibonites (δ^{50}Ti =20.9 ± 2.7‰ [B3]; 12.3 ± 5.6‰ [B5]) and both of them are devoid of radiogenic ^{26}Mg excess (initial ^{26}Al/^{27}Al $<3 \times 10^{-6}$ [B3] and $<8 \times 10^{-7}$ [B5]). B5 is also devoid of radiogenic excess in ^{41}K (initial ^{41}Ca/^{40}Ca$<2 \times 10^{-9}$[3]).

Hibonite in the spinel-hibonite inclusion A4 shows an ultra-refractory REE pattern superimposed on fractionated HREE (Fig. 1). The refractory trace elements, Sc, Zr and Hf are also enriched by factors of >500 compared to CI abundances. This hibonite shows a large enrichment in the neutron-rich isotopes, ^{48}Ca (δ^{48}Ca = 51.0 ± 5.8‰) and ^{50}Ti (δ^{50}Ti = 65.3 ± 8.0‰); no detectable excess in radiogenic ^{26}Mg and ^{41}K was found in it (initial ^{26}Al/^{27}Al $< 1 \times 10^{-6}$ and initial ^{41}Ca/^{40}Ca $< 6 \times 10^{-9}$ [3]). Hibonite in the spinel-hibonite spherule, A3, has a Group II REE pattern superimposed over a smooth fractionated hibonite REE pattern (Fig. 1). However, it does not exhibit strong depletion in Eu and Yb often seen in CM hibonites with Group II pattern. This hibonite has a detectable excess in ^{50}Ti (δ^{50}Ti = 12.3 ± 6.6‰) and is characterized by a radiogenic ^{26}Mg excess with initial ^{26}Al/^{27}Al close to the canonical value of 5×10^{-5}. The very low Ca/K ratio in this hibonite ($\sim 8 \times 10^4$) makes it difficult to identify possible presence of radiogenic ^{41}K excess in it.

The isotopic and trace element data for Murchison hibonites obtained by us are in general agreement with earlier data on CM hibonites [1,2,4,5] and allow us to draw some general conclusions about the genesis of these hibonites. Ultrarefractory trace element pattern has been reported earlier for hibonite in a corundum-hibonite inclusion (GR-1) from Murchison [5] and for "bulk" sample of a hibonite-bearing Murchison inclusion MH-115[6]. These hibonites perhaps represent some of the earliest Solar System condensates. They are devoid of radiogenic isotopic anomalies (no ^{26}Mg and ^{41}K excesses), even though they may have stable isotope anomaly, particularly an enrichment in the neutron-rich isotopes, ^{48}Ca and ^{50}Ti. A similar trend is also seen for most of the hibonites with Group III REE pattern. In contrast, many hibonites with Group II REE pattern, that are often superimposed by a fractionated HREE, have excess radiogenic ^{26}Mg and ^{41}K but with very small or no enrichment in ^{50}Ti. The presence/absence of the short-lived nuclides at the time of formation of the CM hibonites may be explained by postulating either a heterogenous distribution of ^{26}Al (and ^{41}Ca) over very small spatial scale in the early solar system [4,7] or formation of some of the ultrarefractory and refractory hibonites prior to the time when these short-lived nuclides, injected from an external source, found their way into the formation zone of the refractory phases in the nebula.

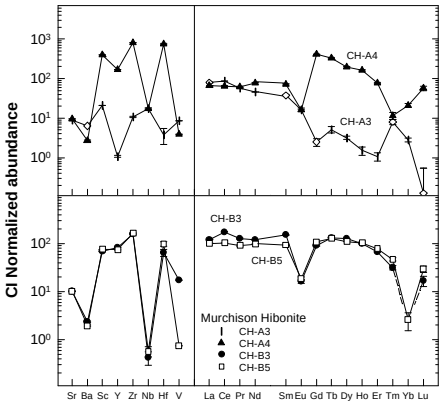

Fig.1. Refractory trace elements and REE abundances in Murchison hibonites.

References: [1] Sahijpal S. et al. (1998) *LPSC XXIX*, #1396, LPI (CD-ROM). [2] Ireland T. R. et al. (1988) *GCA*, *52*, 2841–2854. [3] Sahijpal S. et al. (1998*) Nature*, *391*, 559–561. [4] Fahey A. J. et al. (1987) *GCA*, *51*, 329–350. [5] Hinton R. W. et al. (1988) *GCA*, *52*, 2573–2598. [6] Boynton et al. (1980) *LPSC XI*, 103–104. [7] McPherson et al. (1995) *Meteoritics*, *30*, 365–386.

ABSOLUTE REACTION RATES OF HYDROGEN WITH CONDENSED PHASES IN THE NEBULA. A. Hashimoto, Department of Earth and Planetary Sciences, Hokaaido University, Kita-ku, N10-W8, Sapporo 060, Japan.

A new experimental system has been built that is able to determine absolute reaction rates of gaseous H with various solid and molten substances at high temperatures and low pressures. It is being used to investigate reactions of minerals, chondrules and CAIs with solar nebular gas.

A core part of the new system is a molybdenum tube-cell assembly that consists of a cylindrical Mo cell (L = 82 mm, ID = 22 mm) with the top connected to a Mo inlet tube (L = 500 mm, ID = 7.5 mm), and with the bottom connected to a Mo outlet tube (L = 51 mm, ID = 8.0 mm) which is open to a vacuum. The upper two-thirds of the space inside the Mo cell is loaded with tungsten granules and small strips of tungsten foil; the lower one-third is empty, except from a sample suspended from a thin W/Re wire. The whole assembly, except for the uppermost part of the inlet tube, is set inside a gas-tight alumina tube (L = 800 mm, ID = 55 mm), whose bottom end is connected to a vacuum chamber equipped with a 3000 l/s diffusion pump. The central part of the alumina tube is set inside a high-temperature Deltech tube furnace.

Hydrogen gas was introduced into the Mo inlet tube at a known flow rate. Dissociation equilibrium between molecular and atomic H was attained by many collisions with the catalytic tungsten [1]. A reaction ensued between H and a solid or molten sample. Both H and reaction products were evacuated through the Mo outlet tube into a high vacuum. The weight difference of the sample before and after the experiment and the measured surface area gave the reaction rate of H and the sample material.

This method resolves two contradictory demands: how to remove a reaction product (vapor) from, while providing a reacting gas (H) to, the vicinity of the sample. The H pressure was precisely controlled by using the mass conservation relation, $P_1U_1/T_1 = P_oF_o/T_o$, where: P_1 and T_1 are the temperature and pressure of H inside the Mo cell; U_1 is the gas conductance of the outlet tube; F_o is the controlled flow rate of H in the standard state; P_o of 1 atm, and T_o of 293.15 K. Back reaction of the vapor (recondensation) was minimized by reducing the vapor yield, i.e., by choosing samples with small surface area. Samples with a range of surface areas were used; the measured reaction rates were extrapolated to the zero surface area to eliminate the effect of back reaction. This gave the absolute reaction rate.

Synthetic forsterite (with a porosity of ~30%) was reacted with H at 1500°C. Three different flow rates of H, 6.7, 20.0, and 60.0 SCCM, were used, corresponding to $P_1 = 6.2\times10^{-5}$, 1.87×10^{-4}, 5.61×10^{-4} atm, respectively. Extrapolation of 4 or 5 data points to zero surface area for each pressure condition yielded absolute reaction rates (J_o) of 4.4×10^{-6}, 7.5×10^{-6}, and 1.34×10^{-5} g/cm^{2}s, respectively. From these results, J_o is proportional to the 0.50 ± 0.02 power of P_{H2}, or to the 1.01 ± 0.03 power of P_H if a dissociation equilibrium is complete. A straightforward interpretation is that the actual species that reacts with forsterite is atomic H (unlike the conclusion reached by [2]) and that the reaction rate is governed by Langmuir adsorption equilibrium between atomic H and the solid surface. This is reasonable because the atomic H is by far reactive than the molecular H even if the former abundance is smaller (~1% of the total H at 1500°C and $P_{H2} = 2 \times 10^{-4}$ atm), and because the pressure range studied is well below one atmosphere. Data of Nagahara and Ozawa [2] show widely scattered and systematically low values of reaction rates of forsterite with H compared to present results, because their apparatus did not have good control over several essential parameters (temperature, pressure, and dissociation degree of H, and the degree of back reactions).

References: [1] Moore G. E. and Unterwald F. C. (1964) *J. Chem. Phys, 40,*. 2639. [2] Nagahara H. and Ozawa K. (1996) *GCA, 60,* 1445.

ISOTOPIC MASS FRACTIONATION UNDER SOLAR NEBULAR CONDITIONS. A. M. Davis[1,2], A. Hashimoto[3] and F. M. Richter[2], [1]Enrico Fermi Institute, [2]Department of the Geophysical Sciences, University of Chicago, Chicago, IL 60637 (a-davis@uchicago.edu), [3]Department of Earth and Planetary Sciences, Hokkaido University, Sapporo, Japan.

High temperature evaporation of silicate and oxide melts in vacuum leads to isotopic mass fractionation in favor of heavy isotopes in the residues [1–3]. In a recent experiment [4], melts of Type B Ca-, Al-rich inclusion (CAI) composition were evaporated at 1400°C in the presence of gas at 1 atm and solar nebular oxygen fugacity. The evaporation rate was about 3 orders of magnitude faster than vacuum evaporation. Chemical fractionation occurred, depleting residues in Mg and Si relative to Ca and Al, but producing no isotopic mass fractionation in residues. In order to solve this apparent dilemma, we have conducted new evaporation experiments in H_2 at a pressure more appropriate for the solar nebula, ~10^{-4} atm.

~10 mg samples of melt of Type B CAI composition (10.5 wt% MgO, 29.8% Al_2O_3, 28.4% SiO_2, 30.0% CaO and 1.3% TiO_2) were evaporated in a gas-flow evaporation furnace at 1500°C in the presence of 1.87×10^{-4} atm H_2 [5]. The samples were quenched by turning off the power to the furnace, resulting in a cooling rate of ~50°/min. Some experimental parameters are given in the following table.

Sample	Evap. time (h)	mass loss (%)	Mg loss (%)	Si loss (%)	Evap. rate (g cm^{-2} s^{-1})
H-10	1	16.2	72.9	22.9	3.9×10^{-6}
H-12	1	14.0	70.8	22.9	3.7×10^{-6}
H-13	2	24.2	96.2	40.6	3.3×10^{-6}
H-14	4	32.7	99.2	65.0	2.2×10^{-6}
H-15	8	47.3	99.9	96.4	1.8×10^{-6}

SEM examination showed that H-10 and H-12 contain melilite and glass, with a texture consistent with crystallization from a melt. H-13 appears to have had melilite and melt present at the end of evaporation. The central part of H-14 is melilite, which is surrounded by a fine-grained Ca-, Al-oxide with minor SiO_2. Apparently, a subliquidus breakdown of gehlenitic melilite occurred. H-15 consists entirely of fine-grained Ca-, Al-oxide.

Ion microprobe analyses show that melilite, glass and fine-grained oxides in all samples are enriched in the heavy isotopes of Mg and Si. On plots of mass fractionation vs. % loss for Mg and Si, melilite and glass in H-10 and H-12 fall on the Rayleigh fractionation lines that were determined previously [2] from vacuum evaporation of initially chondritic materials. For H-13 and H-14, melilite plots below the chondritic fractionation lines (i.e., has lower mass fractionation), but glass plots on or above the line. There was too little Mg in H-15 for accurate isotopic measurement, but Si lies near the chondritic fractionation line. It appears that diffusion has limited isotopic equilibration in melilite that was present during evaporation.

It is now clear that isotopic mass fractionation effects do not discriminate between the low-pressure hydrogen reaction-dominated regime and the vacuum evaporation regime. The absence of Mg fractionation effects in the earlier 1 atm experiments [4] must not be due to reaction with hydrogen. Rather, the high pressure in those experiments led to a short mean free path, such that an atom or molecule leaving the surface is likely to hit a gas phase molecule and bounce back to the surface. Recondensation was nearly as fast as evaporation, such that a quasiequilibrium state was achieved. Since there is little equilibrium isotopic mass fractionation at high temperature, the residues were able to chemically fractionate without isotopically fractionating.

Since mass fractionation effects are observed in CAIs and CAIs are thought to form in the solar nebula, it is reassuring that evaporative mass fractionation can occur in the presence of hydrogen. Further work on evaporation rates and isotopic fractionation as a function of temperature and H_2 pressure will allow constraints to be placed on the duration of chondrule and CAI melting in the solar nebula.

References: [1] Davis A. M. et al. (1990) *Nature, 347,* 655. [2] Wang J. et al. (1994) *LPS XXV*, 1457. [3] Davis A. M. et al. (1995) *LPS XXVI*, 317. [4] Richter F. M. and Davis A. M. (1997) *LPS XXVIII*, 1161. [5] Hashimoto A. (1998) *Meteoritics & Planet. Sci.*, 33, this volume.

CHEMICAL AND ISOTOPIC FRACTIONATION DURING EVAPORATION OF A MULTICOMPONENT SYSTEM. H. Nagahara[1] and K. Ozawa[2], [1]Geological Institute, University of Tokyo, Tokyo, Japan (hiroko@geol.s.u-tokyo.ac.jp), [2]Institute for the Study of Earth's Interior, Okayama University, Japan (ozawa@misasa.okayama-u.ac.jp).

Evaporation is a kinetic process that can constrain the time-scale of high temperature events in the solar system that caused chemical and isotopic fractionation. Recent progress in evaporation experiments have provided evaporation rates of major minerals [1–3]. In actual processes, degree of chemical and isotopic fractionation is limited by evaporation rate (J), fractionation factor (K), and diffusion rate (D) of the species in the condensed phase, and incongruent evaporation causes melting and subsequent crystallization in most mineral systems and multi-component systems. The role of those kinetics on chemical fractionation from a multi-component system and their dependence on chemical composition are studied by evaporation experiments with the olivine system. Equilibrium phase relations at low pressures of the olivine system has been studied by [4], which stressed stoichiometric nature of evaporation and the large Mg/Fe distribution between coexisting solid and gas.

The outline of experiments have been shown by [5], where single crystals of olivine from San Carlos were used as a starting material. Crystallographically oriented parallelepipeds were heated in a vacuum furnace at 1400°C, 1450°C, and 1500°C for 6 to about 210 hours. The residue is more magnesian than the initial composition suggesting stoichiometric and incongruent evaporation of olivine at a kinetic condition as well as an equilibrium condition. The average evaporation rate estimated from the weight loss decreases with time; the rate along the c-axis at 1400°C is 0.33 mm/hour in 10 hours to 0.15 mm/hour at 100 hours. Surface composition enriches in MgO and CaO and depleted in FeO and NiO with time. The results show that the olivine looses FeO quickly by evaporation. Interior of a grain is strongly zoned, and the pattern is shallowest along the c-axis and steepest along the a-axis.

Nagahara and Ozawa [6] showed that the development of isotopic fractionation from a congruently evaporating material, such as forsterite, is controlled by the evaporation rate, grain size, and diffusion rate, with a dimensionless parameter, b (=Jr/D). When chemical fractionation is significant, such as the case of olivine, fractionation factor between solid and gas (K) should be one of another important factors that governs the reaction.

We have developed a general equation that describe chemical and isotopic fractionation under the control of diffusion by three parameters, J, D, and K. By using the equation, the experimental results were fitted and the parameters are newly obtained. The results show that J and D should have composition dependence: J along the c-axis varies 8.2E-4 (mm/hr) at Fo_{92} to 4.7E-5 at Fo_{100}, and D along the c-axis 8.0E-11 (cm^2/s) at Fo_{92} and 1.8E-11 at Fo_{100}. If the present dependence of diffusion coefficient on composition is linearly extrapolated to Fo_{86}, the present value is a little smaller than that by [7] and larger than [8]. The evaporation coefficient can be a constant at 0.019 for the (001) and 0.035 at the (100) surface. The equilibrium distribution coefficient of Mg/Fe between coexisting olivine and gas ((XMg/XFe)gas/ (XMg/XFe)solid) at low pressures at 1200°–1600°C is smaller than 0.01 [5], suggesting that the kinetic barrier for evaporation is larger for Mg than Fe from highly magnesian olivine. The present results can be applied to time dependent chemical fractionation of interstellar dusts heated at high temperatures in the solar nebular although the effect of H_2 on K is not known.

References: [1] Hashimoto (1990) *Nature, 347*, 53–55. [2] Nagahara and Ozawa (1996) *GCA, 60*, 1445–1459. [3] Tachibana S. and Tsuchiyama A. (1998) *GCA*, in press, [4] Nagahara H. et al. (1994) *GCA, 58*, 1951–1963. [5] Nagahara H. and Ozawa K. (1998) *LPS XXIX*, 1158–1159. [6] Nagahara H. and Ozawa K. (1997) *LPS XXVIII*, 997–998. [7] Meisener D. J. (1974) *Geochem. Transport Kinetics* (A. W. Hoffman et al., eds.), pp. 117–129. [8] Chakraborty S. (1997) *JGR, 102*, 12317–12331.

MEASUREMENT OF GAS-PHASE SPECIES DURING LANGMUIR EVAPORATION OF FORSTERITE.
R. H. Nichols Jr.[1,2], R. T. Grimley[3], and G. J. Wasserburg[1] [1]Division of Geological and Planetary Sciences, Mail Stop 170-25, California Institute of Technology, Pasadena CA 91125, USA (isotopes@gps.caltech.edu), [2]Present address: Department of Earth and Planetary Sciences Washington University, One Brookings Drive #1105, St. Louis MO 63130, USA (rhn@levee.wustl.edu), [3]Department of Chemistry, Purdue University, West Lafayette IN 47907, USA (rgrimley@wcic.cioe.com).

Forsterite, the most abundant mineral in meteorites, forms at high temperatures often associated with nebular processes. It evaporates congruently, and its equilibrium evaporation is rather well-understood [e.g., 1]. For these reasons, in part, many recent studies have focused on the more difficult kinetics of the free (Langmuir or non-equilibrium) evaporation of this mineral [2–4]. Isotopic fractionations of Mg, Si and O measured in residues of forsterite melts (m.p.~1890°C) have been associated with the evaporation of specific vapor-phase species based on detailed isotopic and mass-balance analyses of the evaporative residues [2–4]. In particular, the isotopic fractionations of Si and O are attributed to kinetic or mass-dependent effects, which many workers have associated with the evaporation of SiO_2 [2–4]. In these studies, however, the identities of the dominant vapor-phase species have not been measured directly, but have only been inferred, and these inferences are not in agreement with what one would expect from equilibrium evaporation where SiO is the dominant Si-bearing species [5]. In this work we have evaporated forsterite at high temperatures in both Knudsen (equilibrium) and Langmuir (non-equilibrium) configurations and have directly measured the atomic and molecular species present in the gas-phase using quadrupole mass spectrometry with an electron-impact ionization source. The dominant Si-bearing species is SiO in both cases.

In the Knudsen configuration, for which preliminary results were previously reported [5], the forsterite sample (solid, Fo_{90}) was cycled from 1300°–1600 °C in 30°–50°C steps. Dominant species detected include Mg, SiO, O, and O_2. Measured SiO/SiO_2 ratios between 100–200 are similar to those observed during the equilibrium evaporation of solid SiO_2 [6] and to those expected from theory. Enthalpies and entropies of reaction computed from van't Hoff plots are in good agreement with those computed from equilibrium thermodynamics for the following evaporation reactions: (1) $Mg_2SiO_4(s,l) = 2Mg(g) + SiO(g) + 3O(g)$, (2) $Mg_2SiO_4(s,l) = 2Mg(g) + SiO(g) + 1.5O_2(g)$, (3) $Mg_2SiO_4(s,l) = 2Mg(g) + SiO_2(g) + 2O(g)$, and (4) $Mg_2SiO_4(s,l) = 2Mg(g) + SiO_2(g) + O_2(g)$.

In the Langmuir configuration, a sample of pure forsterite (Fo_{100}) was heated to temperatures below and above its melting point. Free-evaporation from the solid and liquid produces $SiO/SiO_2 >> 1$ in the vapor-phase, similar to values attained in the Knudsen case. Back-reactions or dissociation of SiO_2 within the experimental apparatus, both of which would tend to enhance the SiO/SiO_2 ratio, are considered to be negligible effects. The present study strongly suggests that Si and O isotopes are mass fractionated by the evaporation from liquid forsterite of SiO and not SiO_2, contrary to inferences by other workers [2–4]. Relative abundances of detected species indicate that forsterite evaporates primarily via the reaction (1) above. The free evaporation rate is significantly lower than the equilibrium evaporation rate, as has previously been noted in the prior mass-loss studies [2–4]. This reduced rate suggests the presence of a kinetic barrier impeding evaporation, for which we calculate an activation energy of 410±33 kJ/mol for Mg and SiO in reaction (1). The results of this study, coupled with the results of [2–4], may preclude simple Rayleigh distillation from an homogenized reservoir as a source for some of the gross isotopic effects observed in laboratory studies of forsterite and possibly in other meteoritic materials.

Acknowledgment: Supported by NASA grant NAGW3337 (GJW). Div. Cont. 8519 (999).

References: [1] Nagahara and Ozawa (1996) *GCA, 60,* 1445. [2] Davis et al. (1990) *Nature, 347,* 655. [3] Hashimoto (1990) *Nature, 347,* 53. [4] Wang (1995) *Ph.D. Thesis,* Chicago, pp. 151. [5] Nichols et al. (1995) *LPS XXVI,* 1047. [6] Porter et al. (1955) *J. Chem. Phys., 23,* 216.

RAYLEIGH DISTILLATION AND CONDENSATION OF POTASSIUM ISOTOPES. T. M. Esat[1] and I. S. Williams[2], [1]Department of Geology, Research School of Earth Sciences, Australian National University, Canberra, ACT 0200, Australia, [2]Research School of Earth Sciences, Australian National University, Canberra, ACT 0200, Australia.

Introduction: In the laboratory, vacuum vaporization of molten silicate samples can duplicate isotope fractionation effects observed in some meteorite inclusions [1-3]. The shift in isotope ratios with mass loss is expected to follow the Rayleigh process and is logarithmically proportional to inverse square root ratio of the masses. Rayleigh distillation demands a well mixed reservoir and the complete removal of the vaporized material.

The rocky planets, the Moon and some meteorites are depleted in elements that are volatile at temperatures below about 1200 K. Large variations in condensation or vaporization temperatures can be invoked to account for the segregation of volatile from refractory elements. Starting with an initial hot nebula, incomplete condensation and removal of uncondensed volatiles is one alternative; partial vaporization and removal of volatiles by heating of cold nebular material is another possibility. Humayun and Clayton [4], have addressed the causes of volatile depletion in planetary materials by searching for mass dependent isotope fractionation in the moderately volatile element potassium. Samples investigated include chondrites, achondrites, lunar samples and two CAIs. The data show normal isotope compositions. Based on this data, Humayun and Clayton rule out Rayleigh type distillation as the cause of volatile depletion. They extrapolate from this point and exclude the possibility of any mass loss due to vaporization. Furthermore, they declare a distinction between "kinetic," Rayleigh type distillation and condensation; asserting that condensation only proceeds through an equilibrium process and with minimal isotope effects. On this basis, they attribute volatile depletion to partial condensation from an initially hot solar nebula. However, based on symmetry arguments both condensation and vaporization are expected to produce similar outcomes and therefore cannot be used to exclude one process over the other as the cause of volatile depletion [5].

Vaporization of K: To investigate the behaviour of K isotopes during high temperature vaporization and condensation we have distilled potassium rich glasses in an RF oven in vacuum ($<10^{-6}$ torr); some of the vapour was collected on stainless substrates. An enclosed Mo tube with a retractable plunger at one end was used to completely vaporize K-glass; the plunger was then inserted to condense the vapour. In primitive, undifferentiated solar system materials potassium often occurs as an alteration reaction product coating high temperature phases; in cracks and vugs as nepheline or sodalite and may be largely of secondary origin. In this sense, potassium rich glass is a reasonable proxy for investigating high temperature behaviour of potassium in the early solar nebula.

Isotopic composition of potassium was measured using SHRIMP II, at mass resolution >5000. Mass loss was determined by weighing and potassium loss by electron probe analysis. Ten residues which lost 0 to 51% of K show an enrichment in ^{41}K relative to ^{39}K from 0 to +17.7 ‰ and match the trend expected from Rayleigh fractionation of mono-atomic K [6]. The evolved vapour phase is enriched in the light K isotope by up to –13‰.

Condensates: The metallic gas from completely vaporized K-glass, collected on a cool stainless surface, consisted mainly of K. Seven measurements along the plunger showed significant heavy K isotope enrichment from +1.2 to +11.2‰. This confirms the expectation [5] that isotopes fractionate during partial vaporization as well as condensation by comparable magnitudes. Therefore, the observed absence of potassium isotope fractionation requires a more complicated scenario than vaporization (condensation) from uniformly mixed liquids (gasses) as the cause of the systematic inner to outer solar system volatile element depletion.

References: [1] Esat T. M. (1988) *Geochim., 52,* 1409–1424. [2] Davis A. M. et al. (1990) *Nature, 347,* 655–658. [3] Lee T. (1977) *Geochim., 41,* 1473–1485. [4] Humayun M. and Clayton R. N. (1995) *Geochim., 59,* 2131–2148. [5] Esat T. M. (1996) *Geochim., 60,* 3755–3758. [6] Yu Y. et al. (1998) *LPSC XXIX*.